Structure and Phase Transitions of Poly(heptamethylene *p,p′*-bibenzoate) As Studied by DSC and Real-Time SAXS/MAXS Employing Synchrotron Radiation

Ginka K. Todorova,[†] Manya N. Krasteva,*[,†] Ernesto Pérez,[‡] José M. Pereña,[‡] and Antonio Bello[‡]

Department of General Physics, Faculty of Physics, University of Sofia, blv. J. Bourchier 5 1164 Sofia, Bulgaria, and Instituto de Ciencia y Tecnología de Polímeros (CSIC), Juan de la Cierva 3, 28006 Madrid, Spain

Received May 20, 2003; Revised Manuscript Received September 26, 2003

ABSTRACT: The structure and phase transitions of liquid-crystalline poly(heptamethylene *p,p′*-bibenzoate) have been studied by DSC and variable-temperature real-time SAXS/MAXS employing synchrotron radiation. It was suggested that three-dimensional crystal order appeared within the smectic domains during cooling the sample because the crystal correlation length is nearly the same as that of the smectic domains. These estimated domain sizes are of the order of the average macromolecular chain length, so that it seems that no chain folding exists in the present case. It was found that SAXS intensity in Porod's region obeys the power law, and it deviates significantly from Porod's law. These deviations were explained by an assumption of anisotropic density fluctuations within the phases. It was supposed that the melting process is ruled by an increasing quantity of anisotropic fluctuations within the crystallites but not by surface melting.

Introduction

Polymer liquid crystals (PLCs) are attracting a great scientific interest in recent years because of their many industrial applications. They are inhomogeneous systems consisting of alternating rigid mesogenic groups and flexible spacers. Their complexity originates from the competition between the mesogenic group alignment and the polymeric tendency to maximize the entropy. Their structure in solid state and the phase transition behavior is not totally understood by now.

Polybibenzoates (PBs) with all-methylene spacers represent an ideal model for investigations of the structure and phase formation of main-chain PLCs. Polybibenzoates with $2 \leq m \leq 10$ form a smectic-type structure (S) on cooling, followed by transition into a three-dimensional crystalline (C) structure.[1−17] However, on heating only members with $m < 7$ exhibit the C−S transition, while members with $m > 7$ undergo a monotropic transition directly into the isotropic (I) melt.[1,4,7,14,15,18] A well-expressed "even−odd" effect has been observed for this class of main-chain LC polyesters concerning thermodynamic parameters of their phase transitions as well as other peculiarities of their structure. Even members form a SA phase, with the mesogens and molecular axes aligned perpendicular to the layer planes, while odd members form alternating S phase (SCA) with molecular axes also perpendicular to the mesogenic layers, but their rigid units are tilted in relation to the normal of mesogenic layers at an angle of about 30° and at opposite directions in the adjacent layers.[1,2,5,6,13,19,20] The layer order of mesogens in the S phase gives rise to one or more orders of diffraction in the X-ray pattern in the middle angle range (MAXS peaks), the position of which depends on the length of the spacers.[1,2,4,7,13−15] Moreover, when the crystal is formed, several diffraction peaks are also usually observed in the MAXS region, at spacings very similar to those for the smectic mesophases. These diffractions arise from the corresponding 00*l* planes of the crystal unit cell.

The object of this study is poly(heptamethylene *p,p′*-bibenzoate) (P7MB). Some studies on the structure and phase transitions of P7MB have been published.[8,14,15,21,22] Our previous time-resolved WAXS results of P7MB confirm that the mesophase is only observed on cooling, since on heating the crystal phase formed from the mesophase undergoes a direct transition into the isotropic state.[22] Moreover, some structural parameters, and its temperature dependence, were determined. The layer spacing of the crystalline phase is rather similar but slightly smaller than that of the mesophase, and crystallization does not change significantly the domain dimensions in the direction perpendicular to the mesogenic layers. It has been hypothesized that the smectic−crystal (S−C) transition within each smectic domain is very similar to the solid-state transition from one crystalline form to another. In other words, well-defined domain boundaries already exist in a smectic phase.[22] Surprisingly, although the crystallization takes place from the already partially ordered S phase, the degree of crystallinity measured by WAXS is rather small, around 30%. Even after long time annealing at high temperatures (150 °C), no more than 50% crystallinity could be reached.[8]

The discussion about the chain folding in smectic and crystalline phases of PLCs is still open. P7MB is a regular semiflexible thermotropic LC polymer. De Gennes suggested for such polymers rapid reversals in molten state in the director to generate hairpins.[23] Later on, Williams and Walter proved theoretically the formation of hairpin defects in semiflexible polymers.[24] Comprehensive morphological studies of PBs strongly suggested the presence of chain fold domains in the smectic

[†] University of Sofia.
[‡] Instituto de Ciencia y Tecnología de Polímeros (CSIC).
* Corresponding author: e-mail manya@phys.uni-sofia.bg.

10.1021/ma0346660 CCC: $27.50 © 2004 American Chemical Society
Published on Web 12/11/2003

phase.[25−28] Tokita et al. supported this assumption on the base of the observed orientation of macromolecules in shear flow of PBs, perpendicular to the shear direction.[27−29] However, no scattering maximum has been detected in the small-angle X-ray scattering (SAXS) pattern of P6MB quenched from the melt.[27,28] This result has been attributed to the disordered stacking of the layer structure. It has been found that the macromolecular orientation in S shear flow of PBs is perpendicular to the shear direction, confirming the lamellar structure of the S phase with defined phase boundaries.[27−29] They supposed that the SAXS reflections, observed after crystallization of P6MB, result from the chain folding that may have already existed in the S phase.

Our unpublished results show that even at isothermal conditions from the melt, at temperatures where the crystal phase is thermodynamically stable, the smectic phase appears first and C phase grows up from the S one by nucleation and three-dimensional crystal growth. In all cases, relatively low degrees of crystallinity are obtained, and the morphology development in the process of the phase transition has not been solved yet.

In this paper, DSC and time-resolved SAXS/MAXS experiments were carried out, using synchrotron radiation, to clarify the morphology and phase transitions of P7MB. Particular attention is paid to the analysis of coherent lengths and to the possible existence of chain folding.

Experimental Section

Materials. P7MB was synthesized by melt transesterification of the diethyl ester of 4,4′-biphenyldicarboxylic acid (bibenzoic acid) and heptamethylenediol. The details of the preparation have been previously reported.[8,14]

Experimental Methods. Size exclusion chromatography data were obtained using a Waters 150C gel permeation chromatograph equipped with two detectors: the conventional refractive index concentration detector and a viscometer Retrofit GPC 150R from Viscotek Co. The universal calibration was obtained from measurements in different polystyrene standards, using chloroform as eluent at 25 °C. The molecular weight values obtained for the P7MB specimen analyzed in this work are $M_w = 76\,000$ and $M_n = 16\,200$.

DSC measurements were carried out in a Perkin-Elmer DSC7 apparatus. Both cooling and heating experiments were performed at a scanning rate of 10 °C/min.

SAXS profiles were obtained at Daresbury Laboratory (station 8.2) using synchrotron radiation. A quadrant detector was employed at a distance of 1.6 m from the sample. Wet rat-tail collagen ($L = 67.0$ nm) was used for calibration. The spacings covered by the experimental setup range were from about 1.5 to 66 nm. The P7MB sample was analyzed in a glass capillary of 1 mm diameter. A Linkam TMS92 temperature controller connected to a THMS600 heating/cooling stage, specially designed for capillaries, was employed. The scattering experiments consisted of successive time frames each recorded typically over a period of 10 s. The corresponding profiles were normalized to beam intensity and corrected relative to an empty capillary background and also for the detector efficiency.

Two scattering ranges of interest are found: (1) a middle-angle X-ray scattering (MAXS) region, covering the approximate range $0.55 \le s \le 0.65$ (Figure 1), where s is the scattering vector, $s = (2 \sin \vartheta)/\lambda$; (2) a small-angle X-ray scattering (SAXS) region (Figure 2), in the range $0.015 \le s \le 0.5$.

From MAXS measurements, the temperature dependences of the mesogenic layer spacing, d_{MAXS}, its integrated intensity, I_{MAXS}, and the domain dimensions in the direction perpendicular to the mesogenic planes, D_{MAXS}, were determined, both for S and C phases, according to Scherrer's formula:

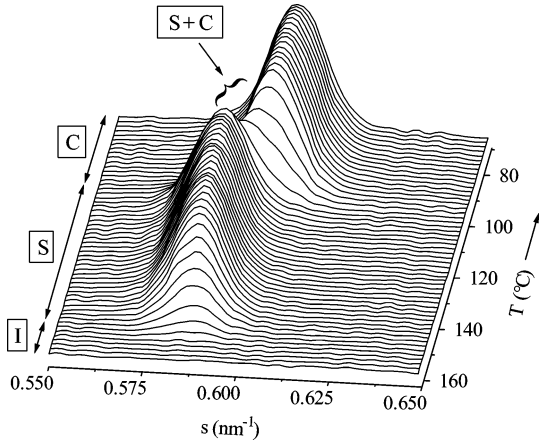

Figure 1. X-ray diffraction profiles, corresponding to the mesogenic layer spacing (MAXS peak), during a cooling experiment of P7MB (cooling rate 10°/min).

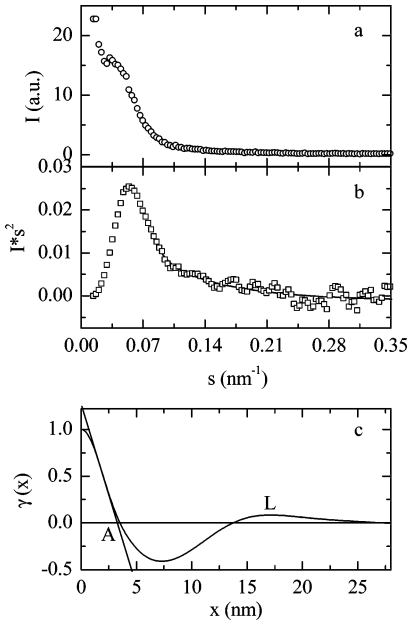

Figure 2. (a) Initial SAXS intensity distribution; (b) Lorentz-corrected curve; (c) one-dimensional normalized correlation function, $\gamma_1(x)$, corresponding to the first frame (74 °C) in a melting experiment.

$$D_{MAXS} = \frac{1}{\delta s} \tag{1}$$

where δs is the full width at half-maximum (FHWM) of the peak. Although the deconvolution of the peaks in the S−C transition range is possible, D_{MAXS} values were not calculated in this region because of higher uncertainty of the value of FHWM.

Long periods were determined from the position of the peak maximum in Lorentz-corrected SAXS patterns, L_{Lor} (Figure 2b), as well as from the first maximum after autocorrelation triangle of the normalized one-dimensional correlation function, $\gamma_1(x)$, calculated according to the equation:[30−32]

$$\gamma_1(x) = \frac{\int_0^\infty s^2 I(s) \cos(2\pi x s)\, ds}{\int_0^\infty s^2 I(s)\, ds} \tag{2}$$

where $I(s)$ is the smoothed and corrected for background SAXS

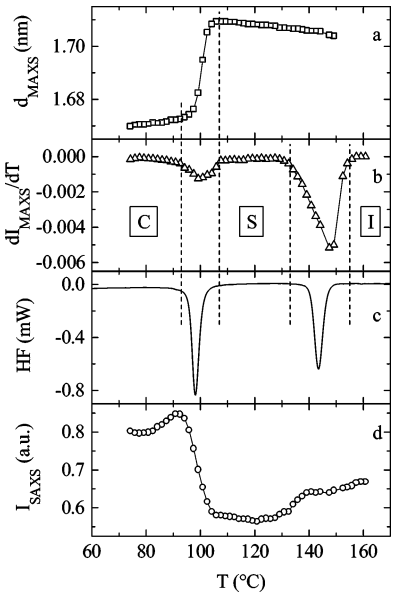

Figure 3. Temperature dependences, on cooling, of (a) d spacing of the MAXS peak, d_{MAXS}; (b) derivative of integrated MAXS intensity, dI_{MAXS}/dT; (c) DSC run; (d) integrated SAXS intensity, I_{SAXS}. Cooling rate 10 °C/min.

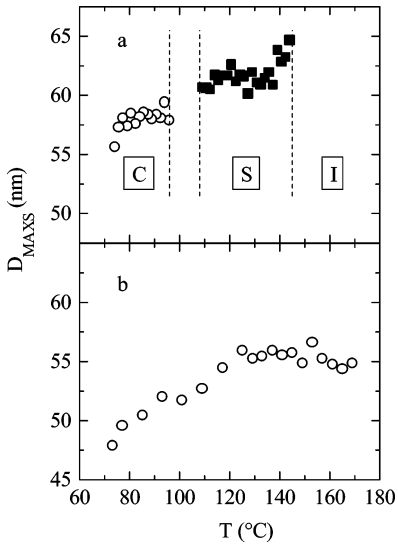

Figure 4. Coherent length, D_{MAXS}, in direction perpendicular to the mesogenic layers vs temperature, evaluated from the FWHM of the MAXS peak: (a) cooling at 10 °C/min. With full squares, D^{S}_{MAXS} in the S phase and with open circles, D^{C}_{MAXS} in the crystalline phase; (b) heating at 10 °C/min.

intensity, obtained after subtraction of the diffuse scattering in the isotropic state at high temperature. It was found (see below) that $I(s)$ in Porod's region obeys the law:

$$I(s) = I_b + \frac{K}{s^n} \tag{3}$$

where I_b is the background intensity, K is a constant, and n was found to be smaller than 4 for all frames and depends strongly on temperature. This deviation from Porod's law will be discussed below. I_b was determined according to eq 3. The extrapolation of SAXS intensity to zero at high s values was not necessary because of the wide range of experimental s values.

The following structural parameters were determined from the analysis of the correlation function:[30,31](1) the long period, L_γ (Figure 2c); (2) the degree of crystallinity within the stacks of lamella, X_{cSAXS}, and the lamellar thickness, l_c, according to the relations[32] (Figure 2c):

$$X_{cSAXS}(1 - X_{cSAXS})L_\gamma = A \tag{4a}$$

$$X_{cSAXS}L_\gamma = l_c \tag{4b}$$

where A is the intersection of the linear regression to the autocorrelation triangle (LRACT) with the x axis; (3) Porod's invariant in arbitrary units, Q, measured from the nonnormalized correlation function, $K(x)$ at $x = 0$ (numerator in eq 2), and Q_{id}, calculated from LRACT to $x = 0$ of $K(x)$ in the autocorrelation triangle.

Results and Discussion

Cooling Process. Figure 3 shows the temperature dependences of d_{MAXS} (Figure 3a), the derivative of the integrated MAXS intensity (Figure 3b), the DSC trace (Figure 3c), and the integrated SAXS intensity (Figure 3d). The temperature dependence of d_{MAXS} has been already discussed in our previous work.[22] Two transitional ranges are clearly observed, corresponding to the isotropic−smectic (I−S) (133 °C < T < 155 °C) and S−C (93 °C < T < 107 °C) transitions. In the first temperature range, a MAXS peak appears, corresponding to the layer spacing of the mesophase, and its intensity gradually rises to a constant value. At lower temperatures, the S−C transition occurs, with an appreciable lowering of the MAXS peak spacing (Figure 3a) changing from around 1.71 nm for the smectic phase to around 1.67 nm for the crystal. A small change is also observed in the total intensity of the peak. The derivative of the MAXS intensity is plotted in Figure 3b: the two transitions are clearly observed, centered at temperatures in perfect agreement with the DSC results (Figure 3c).

Therefore, the smectic MAXS peak disappears when the crystallization occurs, while a new MAXS diffraction peak, corresponding to the crystal, is formed at a slightly lower spacing. Both peaks coexist during the S−C transition. In the present case of P7MB, the two MAXS peaks differ very little in spacing, the difference being smaller than the widths of the peaks, so that the deconvolution in the transition interval involves some uncertainty.

The domain dimensions (the coherent lengths) along the macromolecular axis can be estimated from the width of the MAXS peaks by using Scherrer's equation (see Experimental Section). The results for the cooling process are presented in Figure 4a. It can be observed that the domain size for the mesophase, D^{S}_{MAXS}, is of the order of 61 nm. After crystallization, the crystal domain size, D^{C}_{MAXS}, is slightly reduced: a value around 58 nm is obtained. It seems, therefore, that the crystallization from the mesophase proceeds with very little disruption in the direction of the macromolecular axis of the initial smectic domains.

Formation of stacks of folded lamellar crystals has been suggested previously in the case of P6MB.[26−28] If we assume the same model for P7MB, the number of monomer units, m, per fold, can be evaluated by the relation: $m = D_{MAXS}/d_{MAXS}$. According to this relation, we estimated $m = 36$ in S and $m = 35$ in C domains, which is the same within the experimental errors limit. If we consider that the value of M_n for the present P7MB sample is 16 200 and that the molecular weight of the repeating unit is 338, it means that, on average, around 48 monomeric units are included in a polymer chain. However, the values of D_{MAXS} and m have to be considered as lower limits since no corrections for the

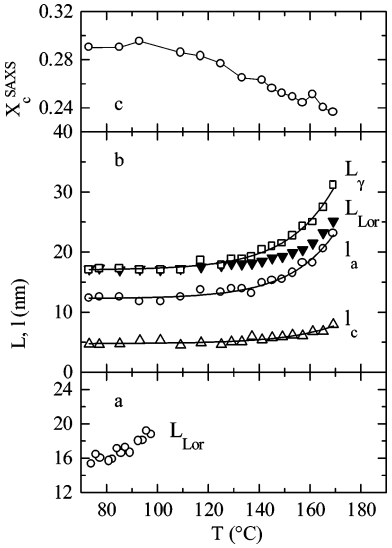

Figure 5. (a) Long period, L_{Lor}, determined by the position of the maximum of the Lorentz-corrected SAXS curve at cooling. (b) Long period, L_{Lor}, determined by the position of the maximum of the Lorentz-corrected SAXS curve at heating (full down triangles) and parameters determined by the one-dimensional correlation function: long period, $L\gamma$ (open squares); thickness of the disordered layers, l_a (open circles); crystal thickness, l_c (open up triangles). Lines are exponential growth functions. (c) Variation of the degree of crystallinity, estimated by SAXS, at heating.

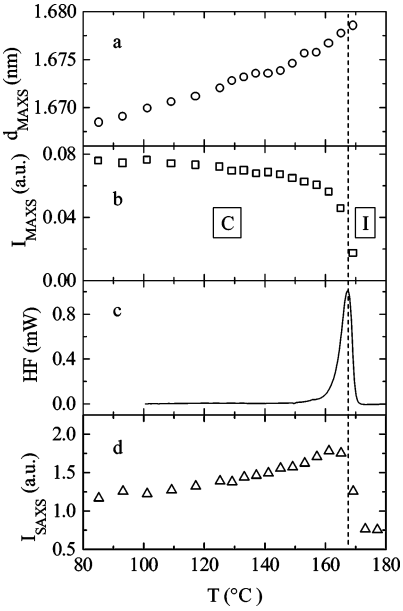

Figure 6. Temperature variation, on heating, of (a) *d*-spacing between mesogenic layers, (b) integrated MAXS intensity, (c) DSC run, and (d) integrated SAXS intensity. Heating rate 10 °C/min.

experimental broadening or for the possible existence of paracrystalline defects have been made.[33,34] Anyway, comparing the number of monomeric units in a chain and the value of *m* (and considering that this represents a lower limit), it follows that we are practically dealing with extended chains, with no chain folding, in the present case of a P7MB with a relatively low molecular weight.

On the other hand, no peak is observed in the SAXS patterns at the temperature range from T_{I-S} to T_{S-C}. This result is similar to the one reported by other authors.[27,28,35] The most probable reasons are either that there is not enough electron density difference between the smectic domains and the amorphous phase or the absence of fully amorphous regions below the I−S transition temperature. Hudson et al. also observed full transformation from the isotropic melt to SCA structure for other odd-number PLC on the basis of phase contrast TEM images.[36] Tokita et al.,[28] on the basis of DSC studies, have also suggested that an overall I−S transformation took place in a short period of time. A noticeable decrease of SAXS intensity just after the I−S transitional range (Figure 3d) would be evidence of homogenization of the structure in the S phase.

However, as expected, the SAXS integrated intensity is very sensitive to the S−C phase transition (Figure 3d). Below the onset of such transition, a SAXS peak with low intensity appears on cooling. The long period, L_{Lor}, decreases slightly when lowering the temperature (Figure 5a), changing from around 19 to 14 nm.

Rodlike structures of stacked lamellae with lamellar thickness of 25 nm have been observed in the crystalline phase of P6MB.[25] The long period has been identified with the lamellar thickness.[27] This statement has been grounded on the very high degree of crystallinity of P6MB. On the contrary, P7MB, as all odd members of PBs, has a relatively low degree of crystallinity (no more than 50%)[5] even after long annealing time. These peculiarities of odd-members PBs behavior were explained by Hudson et al. because the packing constraints in crystal phase produce the molecular chain twisting around each other and cause chain entanglements in the smectic phase. The authors suggested that segregation of entanglements during crystallization limited the crystal growth, causing the lamellar shape of the crystallites.[36]

Correlation functions at cooling can be calculated only for the last frames, when the crystal phase has already formed. All parameters (L_γ, l_{cr}, l_a) are almost constant, excluding the small thermal contraction.

Heating Process. Figure 6 shows the temperature dependences of d_{MAXS} (Figure 6a), the integrated MAXS intensity (Figure 6b), the DSC curve (Figure 6c), and the integrated SAXS intensity (Figure 6d) during heating. Only one transition is seen (centered at 167 °C), attributed to the melting of crystalline phase. This result confirms the monotropic character of the mesophase. The decrease of I_{MAXS} with increasing temperature, accompanied by the increase of crystal size, D^C_{MAXS} (Figure 4b), indicates that some amount of nonequilibrium thin crystals melt much before the maximum in the DSC melting peak. Nevertheless, the most important decrease in I_{MAXS} coincides perfectly with that maximum. On the other hand, d^C_{MAXS} increases linearly with temperature (thermal expansion coefficient $\beta_T = \mathrm{d}(d_{MAXS})/\mathrm{d}T = (0.92 \pm 0.03) \times 10^{-4}$ nm/°C). The value of β_T seems to be somewhat higher in the transition interval ($\beta_T = (1.9 \pm 0.1) \times 10^{-4}$ nm/°C) (which might be due to some extent to simultaneous C−S and S−I transitions).

The different parameters obtained from the correlation functions are shown in Figure 5b,c. Regarding the degree of crystallinity, it can be determined, in principle, from eq 4a. However, this equation is a quadratic one, with two solutions, so that it is not possible to know what is the degree of crystallinity and what is the noncrystal content, unless a certain model or assumption is used. Many authors reported about this uncertainty.[37−42] The problem is, therefore, to decide whether

the minor, for instance, of the two solutions of eq 4a corresponds to the crystal or to the noncrystal content.

If we choose the minor phase as the crystalline phase, the calculated degree of crystallinity decreases slightly from 0.30 to 0.24 when raising the temperature (Figure 5c) and drops sharply in the melting interval. The crystallinity calculated by WAXS is of the same order. However, this is not enough to support the choice we have made since it is possible to have a low overall degree of crystallinity and high linear degree of crystallinity within the lamellae stacks if the volume of the sample is not completely covered by stacks. Nevertheless, the fact that X_c^{SAXS} in Figure 5c decreases on heating (in a similar way that the crystallinity determined by WAXS)[22] allows us to decide that the minor phase is the crystalline one and that lamellar stacks fill completely the space volume. Therefore, the smaller size obtained from the analysis of the γ_1 function can be related to the crystal thickness, l_c.

The variation of L_γ, l_c, and the disordered layer thickness, l_a, with temperature is shown in Figure 5b. L_{Lor} is presented in the same figure with full triangles. At low temperatures the values of L_{Lor} and L_γ coincide, but in the melting interval $L_\gamma > L_{Lor}$. All dependences are exponential growth functions, but l_a shows a higher change with temperature and its contribution to the increase of L_γ is more significant. As was proved on the basis of model calculations,[43] subsequent melting cannot explain the rising of long period at heating and only affects the distribution function of long period and its mean value, while the maximum of the γ_1 function corresponds to the most probable value.[43,44] The recent model calculations,[45] taking into account the initial lamellae thickness distributions, confirm this conclusion. The only model based on one-dimensional periodic structure of polymers that can predict rapid enlargement of L in the melting interval is the "dual lamellar stack" model.[46] According to this model, the structure consists of separated stacks with different long periodicities that melt at different temperatures. However, this model cannot explain the maximum in SAXS intensity during melting (Figure 6d).

On the other hand, l_a shows a higher change with temperature, and its contribution to the increase of L_γ is more significant than that of the lamellar thickness. This dependence supports our choice of l_c to be the smaller size obtained from the correlation function, as such behavior is general for polymers.[45]

The values of l_c are around 5 nm, i.e., drastically different from the crystal coherent length, D^C_{MAXS}, in the direction perpendicular to the mesogenic layers (around 60 nm). The temperature dependences of both parameters are also completely different (Figure 4b and Figure 5b). Moreover, the values of the long period, L, are also considerably lower than D^C_{MAXS} (on both cooling and heating).

Exclusively high correlation lengths along the molecular chains together with smaller lamellar thickness were also reported previously by other authors for semiflexible polymers.[36,46,47] This contradiction was explained by the assumption that crystallization did not influence the coherent length because the S phase was not significantly disrupted by crystallization.[36] The authors observed five different orders of 00*l* diffraction from crystal phase while in the S phase only a 002 peak was visible. However, it is surprising that after such a strong change of the structure the coherent length would remain the same.

Large crystal dimensions and low paracrystallinity along chain axes were found in highly oriented fibers of poly(*p*-phenylene terephthalamide) (Kevlar).[48] The reported value of crystal dimension is 80 nm. After etching Kevlar's fibers in concentrated HCl, lamellae with a thickness of 35 nm were observed in TEM images. These lower values of observed lamellae thickness were explained by the segregation of defects as entanglements and chain ends in layers.

The previous experimental results and our experience with other semiflexible main chain PLCs allow us to conclude that two characteristic lengths exist in partially crystallized samples: the domain coherent length along the macromolecular axes and the crystalline lamella thickness estimated by SAXS. The former size, as a rule, is several times larger than the latter one.

In the case of P7MB, the distributions of SAXS intensity, as well as the shape of the one-dimensional correlation function, are typical for lamellar stacks with quasi-periodic arrangement of nearly parallel lamellae. Hence, the structure is with a real periodic arrangement of lamellae.

The main structural sizes of P7MB are: (1) mesogenic layer spacing (or the length of one monomer unit, MAXS peak), around 1.7 nm; (2) the long period, L, around 17 nm at low temperatures; (3) the domain size in direction perpendicular to the layers, D_{MAXS}, which is of the order of 60 nm; (4) the lamellar thickness, l_c, measured by SAXS, which is around 5 nm. The values (and the temperature dependences) of l_c and D^C_{MAXS} of the crystal are also completely different (Figures 4b and 5b). Moreover, the values of the long period, L, are also considerably lower than D_{MAXS} (on both cooling and heating). How can all these experimental results be incorporated into a single model?

One possible explanation of high values of D^C_{MAXS} on one hand and small values of l_c on the other is that D_{MAXS} could be kept the same after crystallization even if thin crystalline lamellae appear within the mesophase.[36] Accepting this idea, it is impossible to explain the presence of observed SAXS peaks that could be caused by enough electron density difference in that direction.

Another probable hypothesis could be that the periodicity in electron density distribution is not in the direction of macromolecular chains, but perpendicular to them (parallel to the mesogenic layers). This assumption can explain both the observed SAXS peaks and the large differences between the crystal thickness and the crystal coherent length, but it is rather unusual for polymers.

Anyway, further experiments with oriented samples are needed in order to clarify the structure and propose the corresponding model.

The shape of the calculated correlation functions depends strongly on temperature. It is typical for lamellar stacks with a broad thickness distribution.[30−32]

The intersection of $K(x)$, the numerator of eq 2, with the ordinate is proportional to Porod's invariant, Q:[31,32]

$$Q = CX_c(1 - X_c)\langle\Delta\rho\rangle^2 \tag{5}$$

Here, C is the volume fraction of lamellar stacks and $\langle\Delta\rho\rangle$ is the average density difference between ordered and disordered phases. If one assumes that the concen-

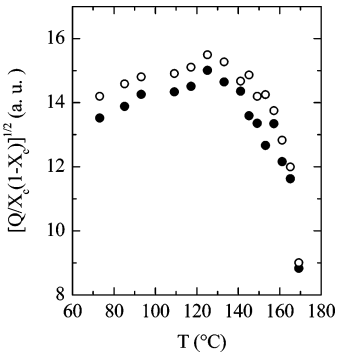

Figure 7. Temperature dependence of the relative average electron difference between ordered and disordered phases: full symbols, calculated from the intersection of unnormalized one-dimensional correlation function, $K(x)$, with y axes; open symbols, calculated from the intersection of linear regression to the autocorrelation triangle with y axes.

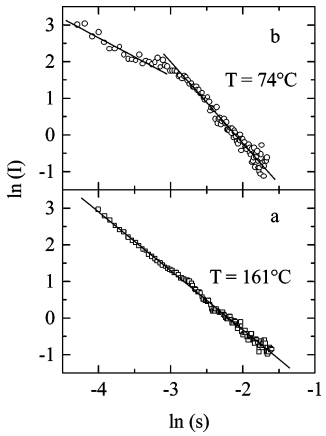

Figure 8. SAXS intensity I_{SAXS} vs s on a double-logarithmic scale: (a) in smectic phase, (b) in semicrystalline phase.

tration of lamellar stacks does not change with temperature, we can find the variation of $\langle\Delta\rho\rangle$ with temperature. This statement is true at low temperatures, but as Goderis et al. proved,[31] the concentration of stacks also decreases in the melting interval. The variation of $[Q/(X_c(1 - X_c))]^{1/2}$ with T is shown in Figure 7. There is no significant difference between $\langle\Delta\rho\rangle$ calculated by Q and by Q_{id}. It is deduced that $\langle\Delta\rho\rangle$ increases gradually with temperature up to the melting interval. This is an evidence of the improvement of the crystal structure and its densification. In this interval, the most probable mechanism of melting is sequential melting of more defect crystals as well as reorganization of the structure inside the crystallites, as the long period does not change significantly. However, the abrupt decrease, observed in Figure 7 in the melting interval up to the isotropization of the structure, can be explained by stack melting (abrupt decrease of C in eq 5).[45]

Deviation from Porod's Law. As is well-known from the theory,[49] the SAXS intensity of semicrystalline polymers with sharp phase boundaries obeys Porod's law when $s \rightarrow \infty$:

$$I(s) \rightarrow (\Delta\rho)^2 \frac{S}{4\pi^3 s^4} \tag{6}$$

where $\Delta\rho$ is the average electron difference and S is the specific internal surface. $I(s)$, on a double-logarithmic scale, is presented in parts a and b of Figure 8 for the smectic and crystalline state, respectively. Only one

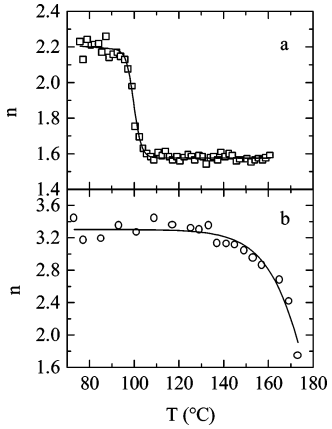

Figure 9. Temperature dependences of the power value, n, of the power law in Porod's region: (a) cooling; (b) heating.

slope is observed in the smectic phase, while two distinct slopes are seen after crystallization. The intercept between these two lines is the lower limit of Porod's region. The slope in this region, n, however, differs significantly from 4. Furthermore, it depends on temperature, as seen in Figure 9, for the cooling (Figure 9a) and heating (Figure 9b) experiments. It is observed that n is independent of temperature in the smectic state and nearly equals 1.6 for all s values (Figure 9a). A similar power law with $n = 3$ of SAXS scattering from the disordered phase was observed by Jonas et al. for PEEK/poly(ether−imide) blends, miscible in the amorphous phase.[40] In the transition temperature range, n rises abruptly and then it seems to increase gradually with lowering the temperature. On heating, n is almost constant with increasing temperature and drops quickly in the C−I transition range. In both cases n is always smaller than the value of 4 predicted by eq 6.

The analysis of some possible deviations from Porod's law was made by Ruland.[50] There are two main reasons leading to deviations from Porod's law: (1) the finite width of the interface and (2) the existence of anisotropic density fluctuations within the phases. In the former case, the intensity is given by:

$$I_{obs} = I(1 - 4\pi^2\sigma^2 s^2) \tag{7}$$

for small values of σs, where σ^2 is the variance of the smoothing distribution perpendicular to the interface. Therefore, considering eq 6, the plot of $I_{obs}\, s^4$ vs s^2 should be a straight line with a negative slope.

On the other hand, two kinds of anisotropic fluctuations within the phases are possible: one- and two-dimensional fluctuations. According to Ruland,[50] for one-dimensional fluctuations $I_{obs}s^4$ vs s^2 should be a straight line with positive slope, proportional to the electron density fluctuations, projected in the direction of fluctuations. In the case of two-dimensional fluctuations, $I_{obs}s^4$ vs s^3 should be a straight line with positive slope, proportional to the density fluctuations, projected onto the plane parallel to the direction of the fluctuation. If it is assumed that the same kind of fluctuations exists in both phases or only fluctuations in one of the phases are significant, the kind of fluctuations could be determined by the relation of Is^4 vs s^2 or s^3. These two dependences are shown in parts a and b of Figure 10, respectively. Both dependences present a positive slope, so that the influence of the fluctuations prevails over the transition layer thickness. It is seen from the

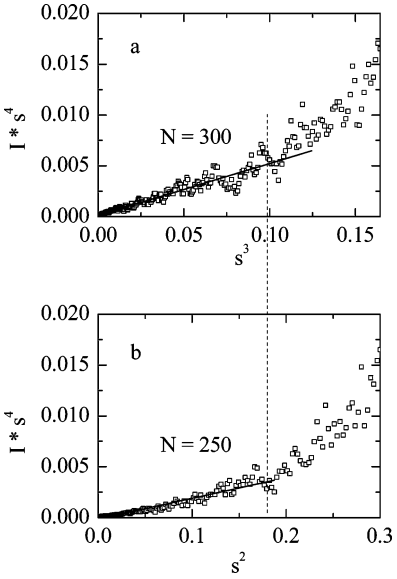

Figure 10. Dependence of (a) $I_{SAXS}s^4$ vs s^3 related to two-dimensional fluctuations; (b) Is^4 vs s^2, related to one-dimensional fluctuations. In the former case, linearity with $R > 0.95$ includes 300 data points; in the latter case, only 250 data points.

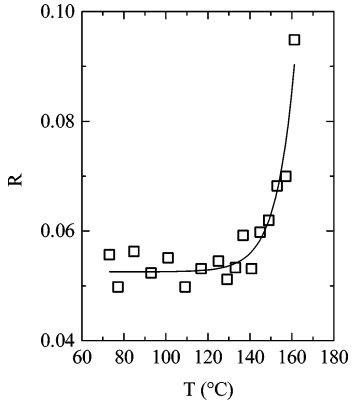

Figure 11. Temperature dependence of the slope, R, of the linear dependence of Is^4 vs s^3, assuming two-dimensional fluctuations into the phase. The line is an exponential growth function.

comparison of both figures that Is^4 vs s^3 is a linear function up to the beginning of the MAXS peak. It can be concluded, therefore, that two-dimensional fluctuations are more realistic in P7MB, although the real situation may be quite more complicated. Nevertheless, the values of the slope R vs temperature, on heating, are presented in Figure 11. It is observed that R increases exponentially above 140 °C, just before the beginning of the melting interval, because of the well-known increase of thermal fluctuations before the melting point. The peculiarity of P7MB is that the fluctuations are anisotropic.

Polymer crystals could melt in two different ways: (1) Surface melting, during which transition layer increases and crystal core becomes smaller and smaller, until its full isotropization. The surface melting is in contradiction with our experimental results, as the average crystal sizes in both directions, perpendicular and parallel to the molecular axes, increase with the temperature. (2) Density fluctuations appear within the crystal phase until the free energy of the crystal phase equals that of the disordered phase. This assumption is in agreement with our results. The origin of fluctuations with two-dimensional anisotropy cannot be clarified only on the basis of SAXS results.

Conclusions

Phase transition intervals and temperatures, determined by X-ray scattering, both SAXS and MAXS, coincide with those determined by DSC.

In the smectic phase of P7MB, the material is organized in domains with correlation lengths of about 60 nm.

After crystallization, the crystal coherent length is nearly the same as that of the smectic domains. It was assumed that three-dimensional crystal order appears within the smectic domains when cooling the sample. Stacks of the crystallites seem to be packed with periodicity along a direction perpendicular to the macromolecular axes. These estimated domain sizes are of the order of the average macromolecular chain length, so that it seems that no chain folding exists in the present case of P7MB.

Long period, disordered and crystal layer thickness, determined from the analysis of the one-dimensional correlation function, increase exponentially with temperature during heating.

It was found that the SAXS intensity in isotropic and smectic phases obeys the power law with power $n = 1.6$.

After crystallization, the SAXS intensity at high s values obeys the power law, and it deviates significantly from Porod's law. These deviations can be explained by the assumption of anisotropic density fluctuations within the phases.

The melting process is ruled by an increasing quantity of anisotropic fluctuations within the crystallites but not by surface melting.

Acknowledgment. We thank the NATO Science Committee for the invited scientist grant awarded to M. Krasteva. The financial support of MCYT Project MAT2001-1731 and Foundation for Scientific Researches of Sofia University under Contract 3452 is also gratefully acknowledged. Dr. W. Bras and the Daresbury laboratory (U.K.) are also thanked for their assistance in the synchrotron experiments.

References and Notes

(1) Watanabe, J.; Hayashi, M. *Macromolecules* **1988**, *21*, 278.
(2) Watanabe, J.; Hayashi, M. *Macromolecules* **1989**, *22*, 4083.
(3) Bello, A.; Pérez, E.; Marugán, M. M.; Pereña, J. M. *Macromolecules* **1990**, *23*, 905.
(4) Pérez, E.; Bello, A.; Marugán, M. M.; Pereña, J. M. *Polym. Commun.* **1990**, *31*, 386.
(5) Pérez, E.; Riande, E.; Bello, A.; Benavente, R.; Pereña, J. M. *Macromolecules* **1992**, *25*, 605.
(6) Pérez, E.; Pereña, J. M.; Benavente, R.; Bello, A.; Lorenzo, V. *Polym. Bull. (Berlin)* **1992**, *29*, 233.
(7) Bello, A.; Riande, E.; Pérez, E.; Marugán, M. M.; Pereña, J. M. *Macromolecules* **1993**, *26*, 1072.
(8) Pérez, E.; Marugán, M. M.; VanderHart, D. L. *Macromolecules* **1993**, *26*, 5852.
(9) Benavente, R.; Pereña, J. M.; Pérez, E.; Bello, A.; Lorenzo, V. *Polymer* **1993**, *34*, 2344.
(10) Bello, A.; Pereña, J. M.; Pérez, E.; Benavente, R. *Macromol. Symp.* **1994**, *84*, 297.
(11) Benavente, R.; Pereña, J. M.; Pérez, E.; Bello, A.; Lorenzo, V. *Polymer* **1994**, *35*, 3686.
(12) Pérez, E.; Marugán, M. M.; Bello, A.; Pereña, J. M. *Polym. Bull. (Berlin)* **1994**, *32*, 319.
(13) Watanabe, J.; Hayashi, M.; Morita, A.; Niiori, T. *Mol. Cryst. Liq. Cryst.* **1994**, *254*, 221.

(14) Pérez, E.; Pereña, J. M.; Benavente, R.; Bello, A. In *Handbook of Engineering Polymeric Materials*; Cheremisinoff, N. P., Ed.; Marcel Dekker: New York, 1997; p 383.
(15) Watanabe, J.; Hayashi, M.; Nakata, Y.; Niori, T.; Tokita, M. *Prog. Polym. Sci.* **1997**, *22*, 1053.
(16) Tokita, M.; Osada, K.; Watanabe, J. *Polym. J.* **1998**, *30*, 589.
(17) Tokita, M.; Sone, M.; Kurosu, H.; Ando, I.; Watanabe, J. *J. Mol. Struct.* **1998**, *446*, 215.
(18) Tokita, M.; Osada, K.; Watanabe, J. *Liq. Cryst.* **1997**, *23*, 453.
(19) Li, X.; Brisse, F. *Macromolecules* **1994**, *27*, 7718.
(20) Li, X.; Brisse, F. *Macromolecules* **1994**, *27*, 7725.
(21) Zamfirova, G.; Krasteva, M.; Misheva, M.; Mihaylova, M.; Pérez, E.; Pereña, J. M. *Polym. Int.* **2003**, *52*, 46.
(22) Pérez, E.; Todorova, G.; Krasteva, M.; Bello, A.; Pereña, J. M. *Macromol. Chem. Phys.* **2003**, *204*, 1791.
(23) De Gennes, P. G. In *Polymer Liquid Crystals*; Ciferri, A., Krigbaum, W. R., Meyer, R. B., Eds.; Academic Press: New York, 1982; Chapter5.
(24) Williams, D. R. M.; Warner, M. *J. Phys. (Paris)* **1990**, *51*, 317.
(25) Takahashi, T.; Nagata, F. *J. Macromol. Sci., Phys.* **1989**, *B28*, 349.
(26) Krigbaum, W. R.; Watanabe, J. *Polymer* **1983**, *24*, 1299.
(27) Tokita, M.; Takahashi, T.; Hayashi, M.; Inomata, K.; Watanabe, J. *Macromolecules* **1996**, *29*, 1345.
(28) Tokita, M.; Osada, K.; Kawauchi, S.; Watanabe, J. *Polym. J.* **1998**, *30*, 687.
(29) Tokita, M.; Osada, K.; Watanabe, J. *Polym. J.* **1998**, *30*, 589.
(30) Vonk, C. G. *Appl. Crystallogr.* 1**973**, *6*, 81.
(31) Goderis, B.; Reynaers, H.; Koch, M. H. J.; Mathot, V. B. F. *J. Polym. Sci., Part B: Polym. Phys.* **1999**, *37*, 1715.
(32) Strobl, G. R.; Schneider, M. *J. Polym. Sci., Part B: Polym. Phys.* **1980**, *18*, 1343.
(33) Alexander, L. E. In *X-Ray Diffraction Methods in Polymer Science*; John Wiley & Sons: New York, 1969; p 424.
(34) Baltá-Calleja, F. J.; Vonk, C. G. In *X-Ray Scattering of Synthetic Polymers*; Elsevier: Amsterdam, 1989; p 138.
(35) Wutz, C.; Stribeck, N.; Gieseler, D. *Colloid Polym. Sci.* **2000**, *27*, 1061.
(36) Hudson, S. D.; Lovinger, A. J.; Gómez, M. A.; Lorente, J.; Marco, C.; Fatou, J. G. *Macromolecules* **1994**, *27*, 3357.
(37) Ivanov, D. A.; Amalou, Z.; Magonov, S. N. *Macromolecules* **2001**, *34*, 8944.
(38) Hsiao, B. S.; Wang, Z.; Yeh, Z.; Goo Y.; Sheth, K. C. *Polymer* **1999**, 3515.
(39) Hsiao, B. S.; Sauer, B. B.; Verma, R. K.; Zachmann, H. G.; Seifert, S.; Chu, B.; Harney, P. *Macromolecules* **1995**, *28*, 6931.
(40) Yonas, A. M.; Ivanov, D. A.; Yoon, D. Y. *Macromolecules* **1998**, *31*, 5352.
(41) Wang, Z. G.; Hsiao, B. S.; Fu, B. X.; Liu, L. J.; Yeh, I.; Sauer, B. B.; Chang, H.; Schultz, J. M. *Polymer* **2000**, *41*, 1791.
(42) Chen, J. C.; Chen, C. C.; Wang, R. C.; Fang, D. M.; Tsai, M. J. *Polymer* **1997**, *38*, 2747.
(43) Crist, B. *J. Polym. Sci., Part B: Polym. Phys.* **2001**, *39*, 2454.
(44) Robelin-Soffache, E.; Rault, J. *Macromolecules* **1989**, *22*, 3581.
(45) Crist, B. *Macromolecules* **2003**, *36*, 4880.
(46) Pope, D. P.; Keller, A. *J. Polym. Sci., Polym. Phys. Ed.* **1976**, *14*, 821.
(47) Panar, M.; Avakian, P.; Blume, R. C.; Gardner, K. H.; Gierke, T. D.; Yang, H. H. *J. Polym. Sci., Polym. Phys. Ed.* **1983**, *21*, 1955.
(48) Kent, S. L.; Geil, P. H. *J. Polym. Sci., Part B: Polym. Phys. Ed.* **1992**, *30*, 1489.
(49) Porod, G.; In *Small Angle X-Ray Scattering*; Glatter, O., Kratki, O., Eds.; Academic Press: London, 1982; Chapter 2, pp 17−51.
(50) Ruland, W. *J. Appl. Crystallogr.* **1974**, *4*, 70.

MA0346660